Fast Finite Time Robust-Adaptive Terminal Sliding Mode Approaches for DFIG wind Turbines in the Presence of Unbounded Perturbations

Seyed Mahyar Mehdizadeh Moghadam[1], Esmail Alibeiki[2*], Alireza Khosravi[3]

Abstract–This paper proposes a new approach of Fast Finite Time Terminal Adaptive Sliding Mode (FFTASM) control for perturbed Dual-Feed Induction Generators (DFIG)-based wind turbines which are exposed to unbounded modeling uncertainties and external disturbances. Two separate FFTASM controllers are designed for both turbine and generator sections. The proposed approach can control the maximum power at low wind speeds in Zone II of the Wind Energy Conversion System (WECS), as well as the generated power in the presence of unknown unbounded perturbation in Zone III. Considering the dependence of the modeling uncertainties and external disturbances on respectively the dynamic parameters of the wind turbine and its status, it is assumed that the upper bounds of the sum of the uncertainties and disturbances are unknown nonlinear functions of the wind turbine state variables. These unknown functions are estimated using stable adaptive rules. The fast finite-time stability is proved using Lyapunov's theorem in both turbine and generator sections. Numerical simulations at the end of the paper confirm the correctness of the designed control approached.

Keywords: **DFIG, Wind turbine, sliding mode, Fast terminal sliding mode, Adaptive control, Parameter uncertainty, External disturbance.**

1. INTRODUCTION

1. 1.literature review

The benefit of renewable energy sources is reducing dependence on fossil fuels, increasing network reliability, and solving environmental problems [1]. Wind energy is widely used around the world to generate clean energy. It is one of the renewable energies that is transformed into mechanical and electrical power using the Wind Energy Conversion System (WECS) [2-3]. Wind turbines which are based on the DFIG, are used more than other kinds of turbines due to their higher electrical energy generation and their more appropriate controllability [4]. In DFIGs, when the electronic power equipment can withstand only 20% to 30% of the total system power, the stability of the power grid is guaranteed [5-6]. In [7-8], the range of operation of WECS is divided into four areas: The first Zone (Zone I) indicates when the wind speed is insufficient to move the wind turbine and thus generate energy. In Zone II, by increasing wind speed, the wind turbine output power increases. The output power is controlled using the Maximum Power Point Tracking (MPPT) algorithm. When the wind speed exceeds the nominal value, the pitch angle will be controlled so that the electrical power of the turbine output is around the nominal value (Zone III). When the wind speed passes the allowable limit, the Turbine shuts down to prevent possible damage to the mechanical components of the turbine system (Zone IV). This paper focuses on Zone II and Zone III. Therefore, the control problem is divided into two part:1) DFIG control for maximizing the produced power and 2) Pitch angle control for adjusting the output power. Among the control methods used to control the DFIG section in the research literature, we can mention Filed Oriented Control (FOC), Neuro- fuzzy sliding mode control [7], Predictive pitch control [8], Adaptive control [9], Fuzzy second order integral terminal sliding mode [10], Optimal control [11-12] and robust control [13-15]. It should also be noted that classical linear controllers cannot guarantee system stability because of the highly nonlinear nature of the wind turbine system [16-18]. Not only for the DFIG section but also typically, for

1 Department of Electrical Engineering, Aliabad Katoul Branch, Islamic Azad University, Aliabad Katoul, Iran.
Email: smehdizadeh@aliabadiau.ac.ir

2* Corresponding Author : Department of Computer Engineering, Aliabad katoul Branch, Islamic Azad University, Aliabad Katoul, Iran.
Email:esmail_alibeiki@aliabadiau.ac.ir

3 Faculty of Electrical and Computer Engineering, Babol Noshirvani University of Technology, Babol, Iran. Email:akhosravi@nit.ac.ir

Received: 2025.01.13; Accepted: 2025.02.24

controlling the angle of inclination of the wind turbine blades, the desired rotor speed is compared to the calculated rotor speed. Since the relationship between pitch angle, wind speed, rotor speed, and aerodynamic power is nonlinear, linear approaches cannot adequately control the nonlinear wind turbine system over a wide operational range [19-21]. This is while the performance of WECS firstly changes under the influence of natural phenomena such as temperature, saturation, and skin effect [22]. Secondly, the DFIG section and the turbine part are exposed to modeling uncertainties, external disturbances, and unknown dynamics. As a result, for controlling WECS, we need a robust nonlinear controller. One of the most popular methods of robust nonlinear control is sliding mode control (SMC) which is robust to parametric uncertainty, internal and external disturbances, and modeling error. [23-26]. In [24], a sliding mode controller is used to achieve maximum output power with the help of load reduction to control an actuator train. In [25], using a sliding mode controller and observer, the generator parametric uncertainty and wind speed changes are estimated, and the wind turbine has a resistant performance against these disturbances. The problem of classic sliding modes is the high-frequency, low-amplitude oscillations called chattering. Various methods have been proposed to reduce the chattering, including using the saturation function instead of the sign function, applying high-order sliding mode, and so on. In [27-28], a fractional order sliding mode for direct power control of grid-connected DFIG is designed, which is responsible for controlling the reactive power of the wind turbine. The authors in [28] compared the classical sliding mode controller to the fractional-order sliding mode controller (FOSMC). They concluded that, although the fractional order controller is more efficient due to the nonlinear nature of the system, the adjustment of the parameter is difficult, and the convergence time to the desired value is also infinite. In controlling the wind turbine system, it is necessary to achieve two goals: improving the maximum output power and tracking the turbine speed. The classic SMC controllers only can guarantee asymptotic stability for systems in which the convergence time of error to zero is theoretically infinite [29-30]. In high-accuracy controllers, we achieve fast convergence only by applying a considerable control input that is not desirable in practice. Terminal sliding Mode (TSM) control is a solution to achieve finite time convergence in wind turbine systems [31]. TSM sliding mode is performed using recursive nonlinear differential equations and has more accuracy and tracking speed than SMC. In the last two or three years, the control engineers have proposed the use of the TSM control method in wind turbines for various purposes (TSM control for voltage sag mitigation in wind turbines [32], Non-singular TSM control using feedback of power and load in [33] and speed control of turbine using TSM control in [34]), however, this problem becomes very complicated and challenging when the system is simultaneously subject to perturbations with unknown upper bands in the form of a nonlinear function with unknown coefficients. Solving this problem is the main innovation of this paper.

1.2. The Main Contribution of this paper

The novelty of this paper and main contribution to the literature can be summarized in three part.

1.2.1. Unknown nonlinear functional upper bound of perturbations

In real applications, the dynamic parameters of wind turbine systems, such as inertial, radius, density, power coefficient, inductance, resistance, and so on, are all supposed to uncertainties. On the other hand, the strong nonlinearity of the WECS system makes these uncertainties to be dependent on the system states including rotor speed or DFIG currents.

Also, the effect of wind (as the primary disturbance) on the wind turbine, depends on its attitude, the length of the blades, or the pitch angle. The same is true about the effect of disturbances governing the DFIG. As a result, the disturbances in the model are also dependent on WECS state variables.

According to the above two paragraphs and by calling the sum of the uncertainties and disturbances as system perturbations, in this paper, unlike other previous research (where the upper bound of perturbations is a constant known value in the most conservative mode), it is assumed that the upper bound of perturbations is an unbounded non-linear function with unknown coefficients of WECS state variables. By solving the problem with this assumption the wind turbine control problem is solved: 1- In both the turbine and generator parts, 2- Without any knowledge of perturbations and their upper bounds, and 3-Even in the presence of unbounded perturbations. The unknown coefficients of the perturbation upper bound function will be estimated by designing stable adaptive laws.

1.2.2.Finite Time stability in the presence of perturbations with unknown upper bunds

The stability proof of finite-time convergence of the errors in the whole WECS system is not simply obtained when the unknown coefficients of the functional upper bound of

perturbations are estimated by adaptive rules. Lyapunov stability proof in the presence of these adaptive laws is the main challenge of this problem. This is the next significant achievement which is obtained and solved in this paper.

1.2.3. Usability of designed FFTASM approach for a wide range of dynamic systems

In the current paper for the generator section: DFIG perturbed model is controlled by input voltage control for achieving the maximum aerodynamic power from the changes in wind speed in Zone II. For *turbine section*: The wind turbine perturbed model is controlled by pitch angle control so that the output speed of the wind turbine tracks a desired value in Zone III.

In this paper, the generator model is deliberately rewritten as a nonlinear first-order equation subject to perturbations and the turbine model is rewritten as a second-order nonlinear model subject to perturbations. Therefore, the FFTAM control ideas designed in this paper can be easily applied to a wide range of different types of nonlinear high-order dynamic systems. The method presented in this paper can be used for the finite-time stabilization of many systems subject to unlimited and unknown disturbances and uncertainties.

To the best of the authors' knowledge, considering the above three items in the control problem of WECS systems has not been done in the previous research and will be discussed in this paper. In this paper, the nonlinear functions with unknown coefficients are assigned to the upper bounds of the perturbations in a DFIG-based wind turbine for Zones II and III. Two separate FFTASM controllers one for DFIG section and one for wind turbine section are then proposed for stabilizing the WECS system. Using the Lyapunov stability and its finite time lemma,finite time stability of the whole WECS system to achieve the maximum power is proven, and this limited time is accurately calculated. In addition, the unknown coefficients of the nonlinear functions assigned to the upper bounds of uncertainties and disturbances are also estimated by designing some stable adaptive laws.

The rest of this paper is organized into six sections: Section 2 deals with some required definitions and lemmas as preliminaries and also WECS system modeling. Problem formulation is presented in Section 3. In Section 4 design of the proposed FFTASM approaches, along with their stability proofs and finite time stability computations, is presented. Section 5 examines the correctness of the performance of the designed control approaches with some numerical simulations. The closed loop system behavior, in the presence of unknown perturbations, is also evaluated in this section. Finally, the conclusion, and some suggestions for further work, is expressed in Section 6.

2.PRELIMINARIES

One definition and two lemmas are presented here as preliminaries.

Definition1: Consider a nonlinear system with the following formula:

$$\dot{x} = f(x,u)\ ,\ f(0,0) = 0\ ,\ x_0 = 0 \tag{1}$$

where $x \in R^n$, $u \in R^m$ and $f : R^{n\times m} \to R^n$. If there is an SFC (state feedback control) law in the form of $u = \Phi(x)$ with $\Phi(0) = 0$, then, the system origin of (1) is finite-time stable if the origin of the closed loop system $\dot{x} = f(x,\Phi(x))$ is in a finite-time stable equilibrium state.

To obtain the main result of the paper, the following lemmas from [35] are also needed.

Lemma1: Assume that $V(x)$ is a candidate Lyapunov function and (2)

$$\dot{V}(x) + \alpha V(x) + \beta V^{\gamma}(x) \le 0\ ,\ \alpha,\beta > 0 \tag{2}$$

and $0 < \gamma < 1$. Then, the Lyapunov function $V(x)$ converges to zero in finite time (3)

$$T_k \le \alpha^{-1}(1-\gamma)^{-1} \ln(1 + \alpha\beta^{-1} V_0^{(1-\gamma)}) \tag{3}$$

Here V_0 indicates the initial condition of the Lyapunov function [36].

Lemma2*:* If we have the following two nonlinear differential relations

$$\begin{aligned} &\dot{x} + \beta |x|^{\gamma} \times sign(x) = 0 \\ &\dot{x} + \alpha x + \textstyle\int_{t-0}^{t} \beta |x|^{\gamma} \times sign(x) = 0 \end{aligned} \tag{4}$$

where, $x \in R$, $\alpha, \beta > 0$, and $0 < \gamma < 1$. Then, for each initial condition $x(0) = x_0$, the state of the system approaches the point $x = 0$ in the limited time T_k , which is respectively obtained as follows for the first and second systems in (4)

$$\begin{aligned} T_k &= \frac{1}{\beta(1-\gamma)} \left|\zeta_{(0)}\right|^{1-\gamma} \\ T_k &= \frac{1}{\alpha(1-\gamma)} ln \frac{\alpha \left|\zeta_{(0)}\right|^{1-\gamma} + \beta}{\beta} \end{aligned} \tag{5}$$

for all $t > T_k$ [37].

3. PROBLEM FORMULATION

3.1 WECS SYSTEM MODELING

3.1.1 Wind turbine model

In wind turbines, kinetic energy is converted into electrical energy by an electrical generator. The wind moves the turbine blades and creates rotational force. The wind turbine consists of tower, rotor, and blades. The rotation of the blades moves the rotor, and thus causes the gearbox to move. The gearbox increases the rotation speed, and eventually the generator converts the rotary energy to electrical energy [7].

Wind speed ($v(t)$) and power factor of wind turbines ($C_p(\lambda,\beta)$) are two essential components influencing the behavior of aerodynamic power of wind turbines, which behavior of turbine output's power factor depends on the changes of two terms of blade pitch (β) and the Tip Speed Ratio (TSR)of the blade (λ).

The aerodynamic power of a wind turbine is denoted as follows [38-39]:

$$P_a = \frac{1}{2} \times \rho \pi R^2 C_p(\lambda,\beta) v^3(t) \tag{6}$$

where R is the wind turbine rotor radius component and ρ is the air density in equation (6). The tip speed ratio is

$$\lambda = \frac{\omega_r R}{v} \tag{7}$$

where ω_r stands for the rotor angular speed. Using (8), one can calculate the torque generated by a wind turbine:

$$T_a = \frac{P_a}{\omega_r}, T_a = \frac{1}{2\omega_r} \rho \pi R^2 C_p(\lambda,\beta) v^3 \tag{8}$$

The power coefficient $C_p(\lambda,\beta)$ has the following equations

$$C_p(\lambda,\beta) = c_1(c_2\Gamma - c_3\beta - c_4) \times e^{-c_5\Gamma} + c_6\lambda,$$
$$\Gamma = \left\{\frac{1}{\lambda + 0.8\beta}\right\} - \left\{\frac{0.035}{\beta^3 + 1}\right\} \tag{9}$$

where the constant parameters are c_1 =0.5175, c_2 =116.1, c_3 =0.41, c_4 =5, c_5 =21 and c_6 =0.0069 .

The expression of the dynamics for the turbine can also be simplified as the following simplified model, which is an equation on wind turbine speed

$$\dot{\omega}_r = \left(\frac{1}{J_t}\right) \times \left(T_a - K_t\omega_r - T_g\right) \tag{10}$$

where T_g , J_t , and K_t are respectively the generator electromagnetic torque, total inertia and external damping.

3.1.2. Pitch actuator model

The structure of the pitch actuator is composed of two parts: mechanical and hydraulic parts. The pitch actuator has to rotate the blades along their horizontal axis. The actuator dynamic can be modeled, as a first-order system, as follows [40]:

$$\tau_\beta \dot{\beta} + \beta = U_\beta, \beta_{\min} \le \beta \le \beta_{\max},$$
$$\left(\frac{d\beta}{dt}\right)_{\min} \le \frac{d\beta}{dt} \le \left(\frac{d\beta}{dt}\right)_{\max} \tag{11}$$

where τ_β, and U_β are time constants associated with the pitch actuator, and the actuator control input. [37] depicts the pitch actuator block diagram. We use the saturation term due to the high-frequency components of the pitch demand spectrum [41].

3.1.3 The DFIG Generator model

DFIG-based wind turbines are capable of four-quadrant active, reactive power, and variable speed performance of about 33% of synchronous speed. The losses of DFIG-based wind turbines are much lower compared to a system based on a fully powered synchronous generator with a full converter, it also reduces the cost of the converter (24% of the total power) and requires less maintenance [5-6].

One can write the electrical equations of the DFIG for the rotor and the stator as follows [42]:

Voltage equations (12):

$$\begin{aligned} v_{sd} &= R_s I_{sd} + \frac{d\phi_{sd}}{dt} - \omega_s \phi_{sd} \\ v_{sq} &= R_s I_{sq} + \frac{d\phi_{sq}}{dt} + \omega_s \phi_{sd} \\ v_{rd} &= R_s I_{rd} + \frac{d\phi_{rd}}{dt} - \omega_r \phi_{rq} \\ v_{rq} &= R_r I_{rq} + \frac{d\phi_{rq}}{dt} + \omega_r \phi_{rd} \end{aligned} \tag{12}$$

Flux equations (13):

$$\phi_{sd} = L_s I_{sd} + MI_{rd}, \phi_{sq} = L_s I_{sq} + MI_{rq}, \phi_{rd} = L_r I_{rd} + MI_{sd}, \phi_{rq} = L_r I_{rq} + MI_{sq} \quad (13)$$

The electromagnetic torque formula is then (14)

$$T_{em} = pM(I_{rd} I_{sq} - I_{rq} I_{sd}) \quad (14)$$

where R_r, R_s, ω_r, and ω_s, respectively, are rotor resistance, stator resistance, rotor pulsation, and stator pulsation. Also L_r, L_s, and M are rotor, stator and mutual inductances, respectively. $p$denotes number of pole pairs of DFIG.

For simplicity, the stator resistance is ignored; and it is assumed that the q-axis is aligned with the stator voltage. Then, we have [42]:

$$\begin{aligned} \frac{dI_{rd}}{dt} &= \frac{1}{\sigma L_r}(v_{rd} - R_r I_{rd} + g w_s \sigma L_r I_{rq} - \frac{M}{L_s}\frac{d\varphi_{sd}}{dt}) \\ \frac{dI_{rq}}{dt} &= \frac{1}{\sigma L_r}(v_{rq} - R_r I_{rq} - g w_s \sigma L_r I_{rd} - g w_s \frac{M}{L_s}\varphi_{sd}) \\ \sigma &= 1 - \frac{M^2}{L_s L_r} \\ T_{em} &= -p\frac{M}{L_s}\varphi_{sd} I_{rq} \end{aligned} \quad (15)$$

where $g = \omega_r / \omega_s$ and $\phi_{sd} = v_s / \omega_s$ denotes the leakage coefficient of generator.

In general, for more efficiency, wind turbines are designed to produce maximum power in different regions II and III of a WECS. According to the four working Zones of the wind turbine, the control objectives are as follows:

3.2. DFIG control objective

The components of the DFIG are controlled for obtaining the maximum output power according to the changes in wind speed in Zone II.

The maximum power point trackingin Zone II and zero active power is achieved by tracking the reference electromagnetic torque and keeping the turbine speed constant at its nominal speed in the third control Zone.

The DFIG stator-side reactive power equation is

$$Q_s = \frac{V_s}{L_s}(\frac{V_s}{\omega_s} - MI_{rd}) \quad (16)$$

If we set the reactive power to zero, then the rotor reference current will be equal to:

$$I_{rd-ref} = \frac{V_s}{\omega_s M} \quad (17)$$

To achieve a unity power factor operation of the wind turbine $Q_{s-ref} = 0$, we must have to set or force the optimal reactive power to zero. Thus, the optimal active power P_{s-ref} is written with neglecting losses as $P_{s-ref} \approx P_{a-opt}$. Also, assuming that the reference power is equal to the reference electromagnetic torque, we have:

$$I_{rq-ref} = -\frac{L_s}{PM\phi_{sd}} T_{ref} \quad (18)$$

Therefore, the aim of controlling a DFIG is to optimize the captured wind energy. It is done when the currents in (15) converge to their references in (17) -(18).

3.3 Speed control objective

For speed controlling, high wind speeds are considered. When the generator speed reaches the nominal speed, the turbine enters the third Zone. Now, if the speed of the generator increases by increasing the wind speed, then the controller adjusts it to the optimal value by regulating the pitch angle and control input. So, the received energy from the wind speed is reduced. The power coefficient is dependent on β and λ. Therefore, to obtain the maximum value of C_p, according to β_{opt} and λ_{opt}. The changes of ω_{r-opt} is dependent on the changes of the wind speed as

$$C_p(\lambda_{opt}, \beta_{opt}) = C_{p-\max}, \omega_{r-opt} = \lambda_{opt} v / R \quad (19)$$

To show the direct effect between two components β and ω_r, first, insert T_a from (8) into the turbine model in (10) and assume $T_g = T_{ref} = T_{opt}$. This will Result:

$$\dot{\omega}_r = \left(\frac{1}{J_t}\right)\left(\frac{A.C_p}{\omega_r} - K_t\omega_r - K_{opt}\omega_r^2\right), A = (\frac{1}{2}\rho\pi R^2 V^3) \quad (20)$$

Then according to (8) and to appear $\dot{\beta}$ in (20), it is necessary to derivate from (20) as in below

$$\ddot{\omega}_r = \left(\frac{1}{J_t}\right)\left(\frac{A\dot{C}_p}{\omega_r} - \frac{AC_p}{\omega_r^2}\dot{\omega}_r - K_t\dot{\omega}_r - 2K_{opt}\dot{\omega}_r\omega_r\right) \quad (21)$$

Given that C_p, which is known as the power factor in the equations, is dependent on λ (blade tip velocity ratio) and β (blade angle) and λ itself is dependent on ω_r and v, therefore, the derivative of the turbine's output power factor (C_p) is calculated as

$$\dot{C}_p = \frac{\partial . C_p}{\partial \beta}.\dot{\beta} + \frac{\partial . C_p}{\partial \omega_r}.\dot{\omega}_r + \frac{\partial . C_p}{\partial v}.\dot{v} \quad (22)$$

Now, substituting $\dot{\beta}$ from (11) into (22), it can be simplified as

$$\dot{C}_p = H + \frac{G}{\tau_\beta}\left(U_\beta - \beta\right) + \frac{\partial C_p}{\partial v}\dot{v}, \quad H = \frac{\partial C_p}{\partial \omega_r}\dot{\omega}_r, G = \frac{\partial C_p}{\partial \beta} \quad (23)$$

Where

$$\dot{C}_p = \frac{\partial C_p}{\partial \omega_r}\dot{\omega}_r + \frac{\frac{\partial C_p}{\partial \beta}}{\tau_\beta}\left(U_\beta - \beta\right) + \frac{\partial C_p}{\partial V}\dot{v} \quad (24)$$

Finally, substituting (23) into (21) results in

$$\ddot{\omega}_r = a + bu_\beta + \Delta C_p \quad (25)$$

where

$$a = \left(\frac{1}{J_t}\right)\left(\left(\frac{A}{\omega_r}\right).\left(H - \frac{G}{\tau_\beta}.\beta\right) + K_t.\dot{\omega}_r - \left(\frac{AC_p}{\omega_r^2}\right)\dot{\omega}_r - 2K_{opt}.\omega_r.\dot{\omega}_r\right)$$
$$b = \left(\frac{1}{J_t}\right).\left(\frac{A}{\omega_r}\right)G\left(\frac{1}{\tau_\beta}\right) \quad (26)$$
$$\Delta C_p = \left(\frac{1}{J_t}\right).\left(\frac{A}{\omega_r}\right)\frac{\partial C_p}{\partial V}\dot{V}$$

The goal of our new control approach in this section is to stabilize the rotor angular speed (ω_r) of the turbine in order to tracks a desired reference value ω_{r-ref} by controlling the blade pitch angle (β) and to achieve the maximum aerodynamic power (P_a) from the changes in wind speed. That means the control input in (25) is $u_\beta(t)$ (the pitch angle input), which should be designed so that output $\omega_r(t)$ tracks the desired speed ω_{r-ref} .

3.4. Problem statement

Term ΔC_p in the wind turbine model in (25) includes the wind velocity and its derivatives which can be totally considered as model uncertainties. To deal with uncertainties, at first, we rewrite the model in (25) in a more compact model as follows:

$$N\ddot{r} + K(r,\dot{r}) = \chi \quad (27)$$

where $r = \omega_r(t)$ is the posture variable of system, $\chi = u_\beta(t)$ is input and we have

$$K(r,\dot{r}) = \frac{-a}{b} - \frac{\Delta C_p}{b}, N = \frac{1}{b} \quad (28)$$

where $a,\ b$ and ΔC_p are nonlinear functions of system variables defined as in (26).

Now, in order to make the problem more applicable, assume that other dynamic parameters in turbine model in (26) including A, J_t, H , and so on are unknown for the designer due to modeling uncertainties. This makes both terms N and $K(r,\dot{r})$ to be exposed to uncertainties.

By rewriting the wind turbine model in (27) as follows

$$\bar{N}\ddot{r} + F(r,\dot{r}) = \chi \quad (29)$$

One can easily combine all the unknown terms of N and $K(r,\dot{r})$ in a new defined function $F(r,\dot{r})$ as follows

$$F(r,\dot{r}) = [N - \bar{N}]\ddot{r} + K(r,\dot{r}) \quad (30)$$

where $\bar{N}$ is an arbitrary constant positive value.

It is emphasized again that in reality wind turbine system modeling involves parametric uncertainties, unmodeled dynamics, and external disturbances. The dynamic parameters of a turbine system, including the inertial, air density, rotor radius, tip speed ratio, and so on, are supposed to be uncertainties.

On the other hand, external effects such as the collision of foreign objects and the wind should be modeled as external disturbances. A new term $d(t)$ must add to turbine model in (29) to denote the mentioned external disturbances like noise or effect of any other unknown external force on the wind turbine blades.

Thus, considering both the external disturbances and parameters uncertainties, the more accurate and applicable model of the wind turbine system in (30) is obtained as

$$\bar{N}\ddot{r} + F(r,\dot{r}) + \Delta F(r,\dot{r}) + d(t) = \chi \quad (31)$$

where $F(r,\dot{r})$ indicates the known nominal parts, $\Delta F(r,\dot{r})$ illustrates the term that includes all of the model uncertainties (such as term $\Delta C_p / b$ in (28)). Sum of noises, bounded external disturbances, and unmodeled dynamics is indicated as $d(t)$. By considering parametric uncertainty and external perturbations as an aggregated vector, equation (31) can be simplified as follows:

$$\bar{N}\ddot{r} + F(r,\dot{r}) + E(r,\dot{r},t) = \chi \quad (32)$$

where

$$E(r,\dot{r},t) = \Delta F(r,\dot{r}) + d(t) \quad (33)$$

Remark 1. $\Delta F(r,\dot{r})$ (Modeling uncertainties) is dependent on the wind turbine system states. Also, the external disturbances are depended on the status of the wind turbine system. The fact, that is neglected and ignored in the previous research for simplicity, is that the effect of wind, depends on the speed of the turbine, its attitude and its blade pitch angle.

On the other hand, in most cases, it is assumed that wind speed or at least its upper bound is known for the control designer. This is while, the awareness of the wind's speed or its upper bound and its derivative are not possible in all cases.

Therefore, in this paper and for the first time, we want to assume that the upper bound of the summation of modeling uncertainties and external disturbances in (33) which is denoted by $E(r,\dot{r},t)$, is not a known or constant value, but an unknown nonlinear function of wind turbine state variables. Moreover, to make this assumption more

$$\left\|\Delta F(r,\dot{r})\right\| \le \sigma h(r,\dot{r}) + \partial \tag{34}$$

realistic and applicable, it is also assumed that the coefficients of this function are unknown and would be calculated via some designed adaptive laws.

To do that, inspired by the assumptions on the uncertainties and disturbances presented in [42], the upper bounds of the modeling uncertainties and disturbances in (33) are assumed to be like (34)and (35)

$$\left\|d(t)\right\| \le \upsilon g(r,\dot{r}) + \varsigma \tag{35}$$

So, the upper bound of $E(r,\dot{r},t)$ in (33) can be calculated as

$$\begin{aligned}&\left\|E(r,\dot{r},t)\right\| \le \left\|\Delta F(r,\dot{r})\right\| + \left\|d(t)\right\| \le \\ &\sigma h(r,\dot{r}) + \partial + \upsilon g(r,\dot{r}) + \varsigma\end{aligned} \tag{36}$$

where σ, ∂, υ and ς are scalar values, and $h(r,\dot{r})$ and $g(r,\dot{r})$ are nonlinear functions. with simplification of (36) one can write:

$$\left\|E(r,\dot{r},t)\right\| \le \delta m(r,\dot{r}) + \gamma \tag{37}$$

where $m(r,\dot{r})$ in a nonlinear function and γ and δ are two unknown real constants.

Dealing with the uncertainties and disturbances was not the only aim of this paper. Instead, the objective is to achieve maximum power in the two main areas of the wind turbine within a *finite time*. Designing a finite time sliding mode control law is not simple when the upper bounds of disturbances and uncertainties are considered as unknown nonlinear functions where the unknown coefficients of these functions are obtained by adaptive laws; because it poses a challenge to prove stability through Lyapunov. This will be discussed in the next section.

The problem formulation for DFIG control part is the same as what is presented here for speed control part which is presented along with the proposed controller design in next section.

4. FFTASM CONTROLLER DESIGN

4.1.Turbine Speed controller design (Pitch control technique)

To design the FFTASM controller, at first the wind turbine tracking error is considered as $\tilde{r} = r_d - r$ where $r = \omega_r(t)$. By applying Lemma2, the sliding mode manifold is defined as (33):

$$s = \dot{\tilde{r}} + \zeta\tilde{r} + k\int_0^t sig(\tilde{r})^{\varepsilon} \tag{38}$$

where $sig(\tilde{r})^{\varepsilon} = \left|\tilde{r}\right|^{\varepsilon} sign(\tilde{r})$ with $0 < \varepsilon < 1$ and $k, \zeta \in R^+$.

In order to assign the sliding manifold to converge to zero, a reaching law is considered as follows [36]:

$$\dot{s} = -\rho s - \mu sig(s)^{\lambda} \tag{39}$$

where ρ and μ are constant positive values and $0<\lambda<1$.

By calculating the first-order derivative of s (38), and considering the right hand side of equation (39), The first proposed FFTASM control law for wind turbine model in (31) in the presence of uncertainties and disturbances is designed as

$$\chi = \bar{N}u + F(r,\dot{r}) \tag{40}$$

where u is as follows

$$\begin{aligned}&u = \ddot{r}_d + ksig(\tilde{r})^{\varepsilon} + \zeta\dot{\tilde{r}} + \rho s + \mu sig(s)^{\lambda} + \\ &\eta sign(s) + \left(\hat{\gamma}\left\|\bar{N}^{-1}\right\| + \hat{\delta}\left\|\bar{N}^{-1}\right\| m(r,\dot{r})\right) sign(s)\end{aligned} \tag{41}$$

where $\hat{\gamma}$ and $\hat{\delta}$ are estimation of unknown parameters γ and δ which are obtained from the following adaptive laws

$$\begin{aligned}&\dot{\hat{\gamma}} = k_2 s^T \left\|\bar{N}^{-1}\right\| sign(s), \dot{\hat{\delta}} = \\ &k_1 s^T \left\|\bar{N}^{-1}\right\| sign(s) m(r,\dot{r})\end{aligned} \tag{42}$$

where $k_1, k_2, k, \mu, \rho, \zeta, \bar{N} \in R^+$ (adaptive gains and controller parameters) are arbitrary positive values, and $0 < \varepsilon, \lambda < 1$. The following theorem is the main result of this section.

Theorem 1. Consider the wind turbine model in (29)-(30)

that is exposed to external disturbances and modeling uncertainties with unknown functional upper bounds as in (32). Then, using the FFTASM controller in (40)-(42), where $k_1, k_2, k, \mu, \rho, \zeta, \bar{N} \in R^+$ and $0 < \varepsilon, \lambda < 1$, the rotor speed $r(t) = \omega_r(t)$ converges to the desired reference value $r_d(t) = \omega_{r-ref}(t)$ in a finite time.

Proof. By replacing the relation (40) in (32) and using the multiplication of the sides in $\bar{N}^{-1}$, one can write

$$\ddot{\tilde{r}} + ksig(\tilde{r})^{\varepsilon} + \zeta\dot{\tilde{r}} + \rho s + \mu sig(s)^{\lambda} + \eta sign(s) .. \\ .. + \left(\hat{\gamma}\left\|\bar{N}^{-1}\right\| + \hat{\delta}\left\|\bar{N}^{-1}\right\| m(r,\dot{r})\right) sign(s) - \bar{N}^{-1}E = 0 \quad (43)$$

Now, a Lyapunov's candidate function is selected in the following form:

$$V = \frac{1}{2}s^T s + \frac{1}{2k_1}\tilde{\delta}^2 + \frac{1}{2k_2}\tilde{\gamma}^2 \quad (44)$$

where $\tilde{\delta} = \hat{\delta} - \delta$ and $\tilde{\gamma} = \hat{\gamma} - \gamma$. Using the first-order derivative of V and considering relations (38) and (43), and using $\dot{\tilde{\delta}} = \dot{\hat{\delta}}$, $\dot{\tilde{\gamma}} = \dot{\hat{\gamma}}$, we have:

$$\dot{V} = s^T \left\{-\rho s - \mu sig(s)^{\lambda} - \eta sign(s) - \right. \\ \left. \left(\hat{\gamma}\left\|\bar{N}^{-1}\right\| + \hat{\delta}\left\|\bar{N}^{-1}\right\| m(r,\dot{r})\right) sign(s) + \bar{N}^{-1}E\right\} \\ + (\hat{\delta} - \delta)s^T \left\|\bar{N}^{-1}\right\| sign(s) m(r,\dot{r}) + (\hat{\gamma} - \gamma)s^T \left\|\bar{N}^{-1}\right\| sign(s) \quad (45)$$

By simplifying (45) and considering $s^T sig(s)^{\lambda} = \|s\|^{\lambda+1}$, $s^T s = \|s\|^2$ and $s^T sign(s) = \|s\|$, one can obtain:

$$\dot{V} = -\rho\|s\|^2 - \mu\|s\|^{1+\lambda} - \\ \eta\|s\| - \delta\|s\|\left\|\bar{N}^{-1}\right\| m(r,\dot{r}) - \gamma\|s\|\left\|\bar{N}^{-1}\right\| + s\bar{N}^{-1}E \quad (46)$$

Now, by the fact that $s\bar{N}^{-1}E \le \|s\|\left\|\bar{N}^{-1}\right\|\|E\|$ and using upper bound of E as in (37), one can write (46) as in below

$$\dot{V} \le -\rho\|s\|^2 - \mu\|s\|^{1+\lambda} - \eta\|s\| - \delta\|s\|\left\|\bar{N}^{-1}\right\| m(r,\dot{r}) - \gamma\|s\|\left\|\bar{N}^{-1}\right\| \bar{N} \\ \|s\|\left\|\bar{N}^{-1}\right\|\left(\delta m(\theta,\dot{\theta}) + \gamma\right) = -\rho\|s\|^2 - \mu\|s\|^{1+\lambda} - \eta\|s\| \quad (47)$$

According to (47), it is proved that the derivative of Lyapunov's candidate function is a negative semi-definite, and therefore the condition of stability is established according to the *Barbalat's Lemma.*

Using Lyapunov theory and Lemma 2, we know that if $s(t)$ tends to zero, naturally the error $\tilde{r}$ will converge to zero in the follow finite time (48)

$$T_{\tilde{r}} = \frac{1}{\zeta(1-\varepsilon)} ln \frac{\zeta|z_0|^{1-\alpha} + k}{k}. \quad (48)$$

This time is not the total finite time of error convergence to zero. This only shows that after converging of system to the sliding surface it takes $T_{\tilde{r}}$ seconds for error to become zero. We have to also compute the convergence time of sliding surface to zero by applying the proposed controller in (41)-(43) (we name this time as T_s). Actually, the total convergence time of error to zero is equal to the sum of T_s and $T_{\tilde{r}}$ ($T_{final} = T_{\tilde{r}} + T_s$).

For this purpose, we must define a new Lyapunov candidate function as follows:

$$V_s = \frac{1}{2}s^T s \quad (49)$$

Differentiating V_s and using (38) and (43), results in

$$\dot{} = s^T \left\{-\rho s - \mu sig(s)^{\lambda} - \eta sign(s) - \right. \\ \left. \left\|\bar{N}^{-1}\right\| + \hat{\delta}\left\|\bar{N}^{-1}\right\| m(r,\dot{r})\right) sign(s) + \bar{N}^{-1}E\right\} \\ -\rho\|s\|^2 - \mu\|s\|^{1+\lambda} - \eta\|s\| - \\ \|s\|\left\|\bar{N}^{-1}\right\| m(r,\dot{r}) - \hat{\gamma}\|s\|\left\|\bar{N}^{-1}\right\| + \|s\|\left\|\bar{N}^{-1}\right\|\|E\| \quad (50)$$

By considering (37), the upper bound of $\dot{V}_s$ is estimated as:

$$\dot{V}_s \le -\rho\|s\|^2 - \mu\|s\|^{1+\lambda} - \eta\|s\| - \\ \hat{\delta}\|s\|\left\|\bar{N}^{-1}\right\| m(r,\dot{r}) - \hat{\gamma}\|s\|\left\|\bar{N}^{-1}\right\| + \\ \|s\|\left\|\bar{N}^{-1}\right\|\left(\delta m(\theta,\dot{\theta}) + \gamma\right) \quad (51)$$

Therefore

$$\dot{V}_s \le -\rho\|s\|^2 - \mu\|s\|^{1+\lambda} - \eta\|s\| - \\ \tilde{\delta}\|s\|\left\|\bar{N}^{-1}\right\| m(r,\dot{r}) - \tilde{\gamma}\|s\|\left\|\bar{M}^{-1}\right\| \quad (52)$$

Given the relations (42), (44), and (52) and according to the adaptive laws and theory of Lyapunov, one can conclude that: , $|\tilde{\delta}| \le \bar{\delta}$ and $|\tilde{\gamma}| \le \bar{\gamma}$, where $\bar{\delta}$ and $\bar{\gamma}$ are real constants , and positive bounded. Thus, equation (52). is rewritten as follows:

$$\dot{V}_s \le -\rho\|s\|^2 - \mu\|s\|^{1+\lambda} - \eta\|s\| - \left|\bar{\delta} m(\theta,\dot{\theta}) + \bar{\gamma}\right|\|s\|\left\|\bar{N}^{-1}\right\| \quad (53)$$

Now, given that $m(\theta,\dot{\theta})$ and $\bar{N}^{-1}$ are bounded known values, and $\left|\bar{\delta} m(\theta,\dot{\theta}) + \bar{\gamma}\right|\left\|\bar{N}^{-1}\right\| \le \xi$ yields, so

$$\dot{V}_s \le -\rho\|s\|^2 - \mu\|s\|^{1+\lambda} - \eta\|s\| + \xi\|s\| \quad (54)$$

Now, selecting $\eta > \xi$ and defining $\rho_n = \eta - \zeta > 0$, (54) can be rewritten as

$$\dot{V}_s \le -\rho\|s\|^2 - \mu\|s\|^{l+\lambda} - \rho_n\|s\| \le -\rho\|s\|^2 - \mu\|s\|^{l+\lambda} \quad (55)$$

By substituting $\|s\| = \sqrt{2V_s}$ in (55) and according to (49), one can conclude that

$$\dot{V}_s \le -2\rho V_s - 2^{1+\lambda/2}\mu V_S^{1+\lambda/2} \tag{56}$$

Using Lemma 1 and based on the Lyapunov function in (49), the stability condition is established. The sliding surface converges to the origin in the following finite time:

$$T_s \le \frac{1}{\rho(1-\lambda)} Ln\left(1+\frac{2\rho.V_0^{\frac{(2+\lambda)}{4}}}{2^{\frac{(2+\lambda)}{4}}.\mu}\right) \tag{57}$$

This means that the finite time convergence of error to zero and the finite time convergence of sliding surface to zero (the reaching time) are met. Therefore, the tracking error $\tilde{r}$ converges to zero in the following finite time ($T_{final} = T_{\tilde{r}} + T_s$)(58):

$$T_{final} = \frac{1}{\zeta\times(1-\varepsilon)} Ln\frac{\zeta|\tilde{r}_0|^{1-\varepsilon}+k.}{k.} + \frac{1}{\rho\times(1-\lambda)} Ln\left(1+\frac{2\left(\rho V_0^{\frac{(2+\lambda)}{4}}\right)}{2^{\frac{(2+\lambda)}{4}}\mu}\right). \tag{58}$$

Remark 2. The SIGN function in the FFTASM in (40)-(42) causes high-frequency fluctuations called *chattering* in the control signal. This phenomenon occurs due to the discontinuous sign function in the control law. Chattering damages the mechanical parts of the wind turbine. So far, several solutions have been used to reduce chattering, including utilizing a saturation or hyperbolic tangent function instead of a sign function. However, such replacements reduce the optimal performance of the controller in the closed loop system. To solve this problem, a continuous approximation for the sign function in [44] is proposed. Similar to what was proposed in [44], we also suggest an idea in this regard: Consider the following approximation for the term $\rho\,\mathrm{sgn}(S),\ \rho>0$.

$$\rho\,\mathrm{sgn}(s) \cong \frac{\rho^2 s}{\rho\|s\|+\sigma(\mathrm{t})} \tag{59}$$

where σ(t) is a bounded positive function, that means $\sigma(\mathrm{t})>0$ and $\int_0^\infty \sigma(\mathrm{t})dt<\infty$. Consider the following function as an example of $\sigma(\mathrm{t})>0$:

$$\sigma(t)=\frac{1}{1+t^n}, n\ge 2 \tag{60}$$

It is worth mentioning that using the approximation in (59), firstly the discontinuous sign function will turn into a continuous function. Secondly, this approximation will immediately converge to the sign function itself by maintaining continuity and consumedly the performance of system does not decrease.

4.2. DFIG controller Design(Current control technique)

The assumptions to achieve finite time stability, considering unknown functional upper bound of modeling uncertainties and external disturbances, which were considered in the previous section, are also valid for the DFIG control part. The only difference is that the dynamic model of DFIG part in (12) was of order one, while the wind turbine model in the previous section in (30) was second order.

DFIG model in (12) can be simplified as follow

$$\dot{I}_{rd} = n_{rd} + h.v_{rd}, \dot{I}_{rq} = n_{rq} + h.v_{rq} \tag{61}$$

where

$$n_{rd} = \left(\frac{1}{\sigma.L_r}\right)\times\left(-R_r.I_{rd} + S.\omega_s.\sigma.L_r.I_{rq}\right) \tag{62}$$

$$n_{rq} = \left(\frac{1}{\sigma.L_r}\right)\times\left(-R_r.I_{rq} + g.\omega_s.\sigma.L_r.I_{rd} - g.\omega_s.\left(\frac{M}{L_s}\right).\varphi\right)$$

$$,h = \left(\frac{1}{\sigma.L_r}\right)$$

To prevent repetition, the generator currents I_{rd} and I_{rq} are controlled separately to achieve the maximum power, we write both equations in (61) in an identical format as in below. The stabilizing controller that will be designed later also has the same form for both of these equations:

$$\dot{I} = n + h.v \tag{63}$$

Considering $r = I(t)$ as posture variable of the DFIG system and $\chi = v$ as input, similar to (29)-(30), the DFIG model in (62) can also be written as follows

$$\bar{N}\dot{r} + F(r) = c \tag{64}$$

where $\bar{N}$ is an arbitrary constant positive value and

$$K(r) = \frac{-n}{h} - \frac{d_2}{h}, N = \frac{1}{h}, F(r) = [\frac{1}{h} - \bar{N}]\dot{r} + \frac{-n}{h} - \frac{d_2}{h} \tag{65}$$

The dynamic model of DFIG in (63) is exposed to perturbations such as uncertainties in dynamic parameters like R_r, L_r, g, σ, and so on or also external disturbances like noise, unknown currents, or even undesirable changes in stator speed. Therefore, the more accurate and applicable model of DFIG in (64) should be written by the following equation:

$$\bar{N}\dot{r} + F(r) + \Delta F(r) + d(t) = \chi \tag{66}$$

where $\Delta F(r)$ is model uncertainty and $d(t)$ denotes external disturbance. Similar to (32), the DFIG model can also be stated as

$$\bar{N}\dot{r} + F(r) + E(r,t) = \chi \tag{67}$$

where

$$E(r,t) = \Delta F(r) + d(t).. \tag{68}$$

Note 1. A comparison of equations in (32) and (67) shows that the turbine model and DFIG model can be written similarly and in the same format, with only one-degree difference.

Now, using Remark 1, let us consider the upper bound of external disturbances, and parameter uncertainties in the DFIG system as a nonlinear function of DFIG variables with unknown coefficients as:

$$\left\|E(r,t)\right\| \le \delta m(r) + \gamma \tag{69}$$

where $m(r)$ is a known nonlinear function and γ and δ are unknown real constants.

Considering the tracking error as $\tilde{r} = r_d - r$ where $r_d = \{I_{rd-ref}, I_{rq-ref}\}$ is desired values in (17)-(18), and the sliding mode manifold for the DFIG system based on Lemma 2, is selected as:

$$s = \tilde{r} + k\int_0^t sig(\tilde{r})^{\varepsilon} \tag{70}$$

where ε and k are the same as for (43). Now, similar to what is done for pitch control in the previous part, the fast terminal adaptive SMC for maximizing the produced power in DFIG is suggested as follows:

$$\chi = \bar{N}u + F(r) \tag{71}$$

where u is as follows

$$\begin{aligned} u = {} & \dot{r}_d + ksig(\tilde{r})^{\varepsilon} + \rho s + \mu sig(s)^{\lambda} + \\ & \eta sign(s) + \left(\hat{\gamma}\left\|\bar{N}^{-1}\right\| + \hat{\delta}\left\|\bar{N}^{-1}\right\| m(r)\right) sign(s) \end{aligned} \tag{72}$$

In result χ (73)

$$\begin{aligned} \chi = {} & \bar{N} \times \left\{ \begin{array}{l} \dot{r}_d + ksig(\tilde{r})^{\varepsilon} + \rho s + \mu sig(s)^{\lambda} + \eta sign(s) \\ \quad + \left(\hat{\gamma}\left\|\bar{N}^{-1}\right\| + \hat{\delta}\left\|\bar{N}^{-1}\right\| m(r)\right) sign(s) \end{array} \right\} \\ & + [\frac{1}{h} - \bar{N}]\dot{r} + \frac{-n}{h} - \frac{d_2}{h} \end{aligned} \tag{73}$$

where $\hat{\gamma}$ and $\hat{\delta}$ are obtained from

$$\begin{aligned} \dot{\hat{\gamma}} &= k_2 . s^T \left\|\bar{N}^{-1}\right\| sign(s) \ , \\ \dot{\hat{\delta}} &= k_1 . s^T \left\|\bar{N}^{-1}\right\| sign(s) m(r) \end{aligned} \tag{74}$$

where $k_2., k_1. \in R^+$ are arbitrary positive definite values.

By replacing the relation (67) in (71) and using the multiplication of the sides in $\bar{N}^{-1}$, one can write

$$\begin{aligned} & \dot{\tilde{r}} + ksig(\tilde{r})^{\varepsilon} + \zeta\tilde{r} + \rho s + \mu sig(s)^{\lambda} + \eta sign(s) + \\ & \left(\hat{\gamma}\left\|\bar{N}^{-1}\right\| + \hat{\delta}\left\|\bar{N}^{-1}\right\| m(r)\right) sign(s) - \bar{N}^{-1}E = 0 \end{aligned} \tag{75}$$

Theorem 2*:* Given the DFIG model for both I_{rd-ref} and I_{rq-ref} as in (64), where the upper bound of disturbances and uncertainties is an unknown nonlinear function as in (70). Now, applying the FFTASM controller in (71)-(73), where $k_1, k_2, k, \mu, \rho \in R^+$ and $0 < \varepsilon, \lambda < 1$, the reactive power converges to zero and MPPT is achieved in finite time.

Proof: At first it should be said that converging the DFIG currents to their desired values as in (17) -(18) in finite time, is equivalent to zeroing the reactive power and achieving MPPT in the second control Zone of the wind turbine in finite time. The rest of the proof is similar to Theorem 1 and for the sake of brevity is omitted here.

Remark 3. The wind turbine and the DFIG models in (27) and (64) respectively, have been written in a general form to show that the FFTASM controller can be easily used for other high-order models including all rigid body dynamic models such as robot systems.

Note 2. It is worth to mention that the adaptive rules in equations (42) in Theorem 1, and (74) in Theorem 2, are not only some simple estimations of some parameters ($\hat{\gamma}$ and $\hat{\delta}$) which are used in the control rules (41) in Theorem 1, and (73) in Theorem 2. These adaptive rules are instead the estimations of the unknown coefficients of the functional upper bounds of modelling uncertainties and external disturbances in (37) and (69). In other words, the adaptive rules in (42) estimate the unknown coefficients of the functional upper bound of the wind turbine perturbations in (37) and the adaptive rules in (74) also estimate the unknown coefficients of the functional upper bound of the DFIG perturbations in (69). This is another difference between our work and what is presented in previous researches.

5. SIMULATION RESULTS

This section investigates the performance of the proposed controllers. The designed controller is implemented in MATLAB / Simulink environment. The pitch angle and a double-fed induction generator (DFIG) are controlled by applying the FFTASM algorithm.

The parameters of the wind turbine and the DFIG are reported in Table .1. During the simulation, we use the following functions for external disturbance and parameter

uncertainties in (33) and (69):

$$\Delta F(r,\dot{r}) = af(r,\dot{r}) + 2.1\|r\| + 2.6\|\dot{r}\|$$
$$d(t) = 0.6\sin(0.2t) + 2a \quad (76)$$

where $\Delta F(r,\dot{r})$ illustrates model uncertainties (which includes term $\Delta C_p/b$ in (28)). The ΔC_p and $d(t)$ are plotted in Fig.1(c) and Fig.1(b). where a is a random value between 0 and 1. Fig.1(a), demonstrated the wind speed behavioral variation slopes at different times. The validation of the proposed controller performs under different wind speeds, which vary between 7 to 10 m/s.

Model of the wind is obtained via the following equation

$$V_w = \mu_h + v_t(t).a \quad (77)$$

where μ_h is the average wind speed and v_t(t) represents its instantaneous velocity (instantaneous wind turbulence). The instantaneous velocity of the wind is usually expressed by a first-order filter along with the Gaussian white noise as follows.

$$\dot{v}_t(t) = -\frac{1}{T}.v_t(t) + a_t \quad (78)$$

where T and a_t are the time constant and the white Gaussian noise with zero mean and a specific variance, respectively.

Table 1: Parameters of Turbine and DFIG

DESCRIPTION	PARAMETERS	VALUE
Moment of inertia	J_t	**4.4533E5 KG.M2**
Air Density	ρ	**1.226 KG/M3**
Rotor radius.	R	**3 M**
Rotor inductance	L_r	**0.081 H**
Stator inductance	L_S	**0.084 H**
Rotor resistance	R_r	**0.62 Ω**
Stator inductance	L_s	**0.084 H**
Mutual inductance	M	**0.087 H**
Constant value	σ	**0.1**
Constant value	g	**5.4**

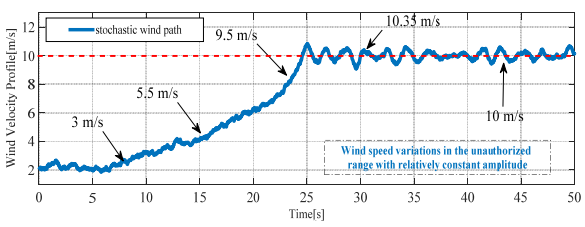

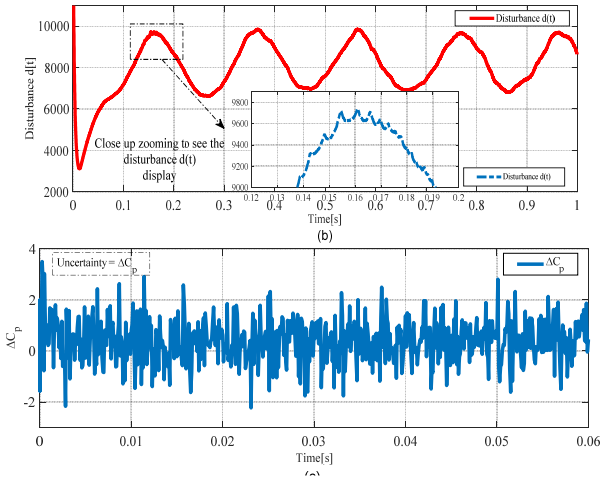

Fig. 1.behavior of wind speed variation slopes at different times(a), The external disturbance(b) and The ΔC_p(c).

To validate the FFTASM control strategy, we used three tests such as step dynamic signal $(\omega_{r-ref}, T_{em-ref}, Ps_{-ref})$, stair sequential dynamic signal $(\omega_{r-ref}, T_{em-ref}, Ps_{-ref})$ and sinusoidal dynamic signal $(\omega_{r-ref}, T_{em-ref}, Ps_{-ref})$. We use Theorems 1 and 2 to select control parameters as follows:

$$\mu = 0.2, \rho = 3.1, k_1 = 0.2, k_2 = 0.3,$$
$$k = 22, \varepsilon = 0.8, \eta = 0.1, \bar{K} = 0.11 \quad (79)$$

The simulations results are shown in Fig.2- Fig.7. Fig.2(a) and Fig.2(b) show the rotor angular speed and the active power, respectively. The angular speed of a wind turbine rotor and the active power output of the generator converge to their reference values for different reference profiles in finite time. From Fig.2(a) and Fig.2(b), it is easy to see that, using the FFTASM in (40), the rotor speed converges to its optimum value $\omega_{ref} = \lambda_{opt} V/R$ in different profiles (Fig.1(a)). Also, the rotor speed is robust against external disturbance and parameter uncertainty in (33). Figs. 2(e) and 2(f) depicts the electromagnetic torque (T_{em}) along with reference torque (T_{em-ref}) in different profiles.

After 0.3 seconds (transition phase), the amount of reactive power becomes zero and remains at this value. That means imposing a unity power factor (Fig.3). Figs.2(c),2(d) and Fig.3 clearly show that with disturbances and uncertainties, with large amounts dependent on system modes, DFIG control in different profiles (Fig.1(a)) is well done. Reactive power is zero, and active power is converged to its reference value.

As expected, these torques converge on each other. It should be emphasized that only in the initial phase, due to significant fluctuations, the electromagnetic torque is not produced commensurate to the captured power, and there is no such problem during the reference change.

In addition, it should be noted that the outputs of the control system which is pitch angle and DFIG voltages are all shown in Figs.4(a) and 4(b). As it is shown, the control efforts are also bounded in both wind turbine and generator control systems.

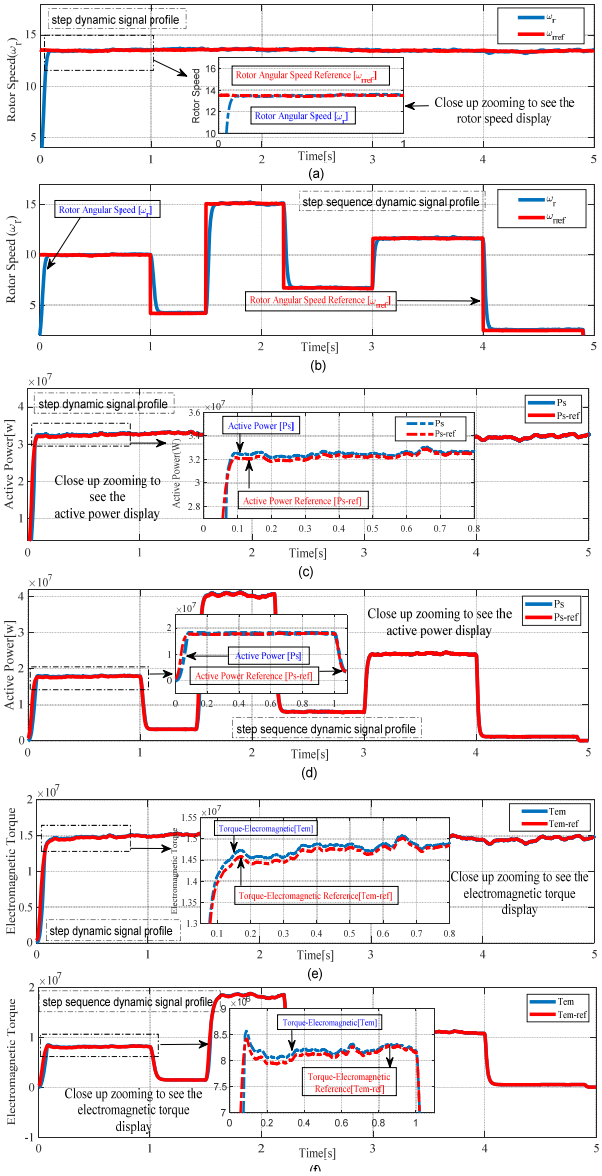

Fig. 2. Rotor angular speed based on step dynamic signal profile(a)&step sequence dynamic signal profile(b) , The active power based on step dynamic signal profile(c) & (b) and step sequence dynamic signal profile(d) and The electromagnetic torque based on step dynamic signal profile(e)&step sequence dynamic signal profile(f)

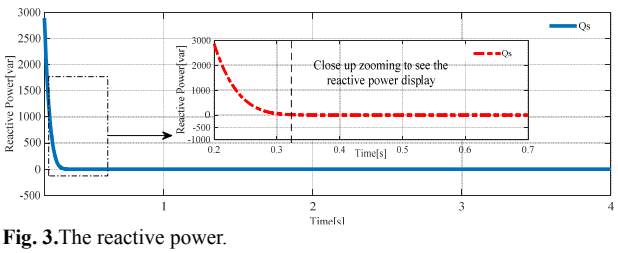

Fig. 3. The reactive power.

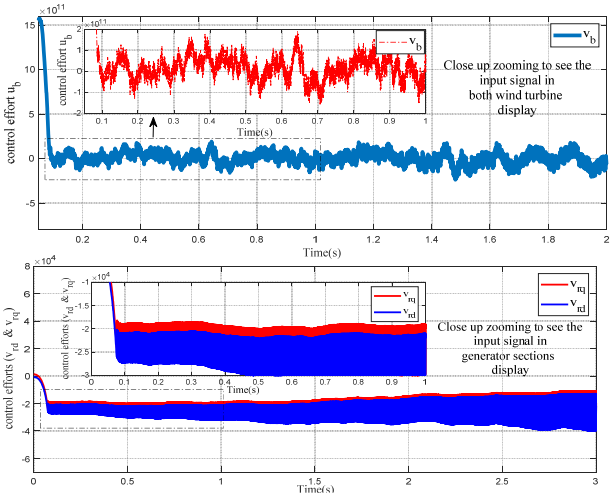

Fig. 4. Input signal in both wind turbine (a) and generator sections(b)

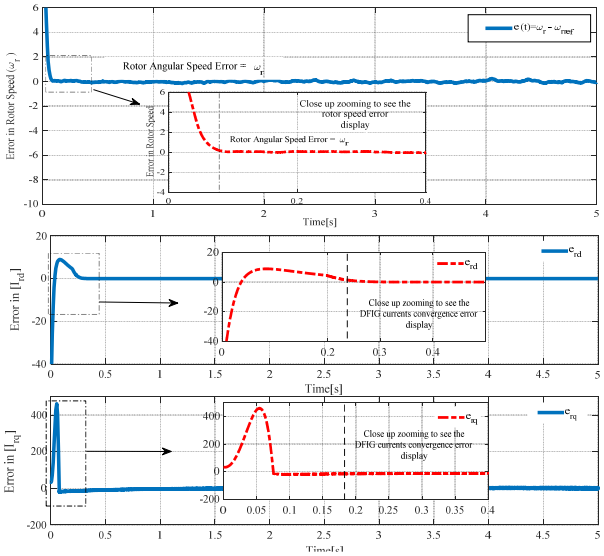

Fig. 5. Rotor speed (a) and DFIG currents (b) convergence error.

The errors related to the convergence of the rotor speed and generator currents to the reference values in the rotor and generator parts are shown in Fig. 5(a) and Fig.5(b). It is cleared that MPPT is achieved by applying the well-designed control law in (40) - (42) and (71) -(74). Fig.6(a) and Fig.6(b) show the behavior of the switching surface of the turbine and doubly-fed induction generator (DFIG) based on parameters S_d , S_q and $S_{(t)}$. As seen in Fig.6(a) and Fig.6(b), the chattering phenomenon has been eliminated, and the sliding surfaces have converged to zero in a finite time. Also, the convergence time, according to Fig.6(a) and Fig.6(b), is less than 0.2 seconds.

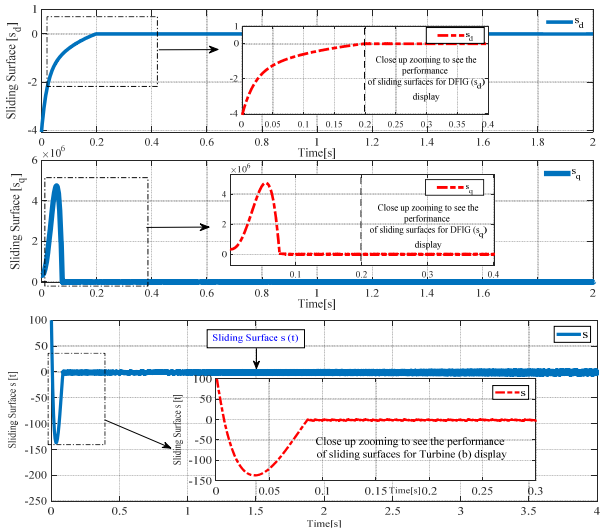

Fig. 6. The performance of sliding surfaces for DFIG (a) and Turbine (b).

Fig. 7 (a, b, and c) shows the adaptive parameters in (42) and (74). It is clear from the stability conditions in the FFTASM controller, the value of adaptive parameters must be limited throughout the simulation. Fig. 7 shows that the adaptive parameters have limited values, as expected.

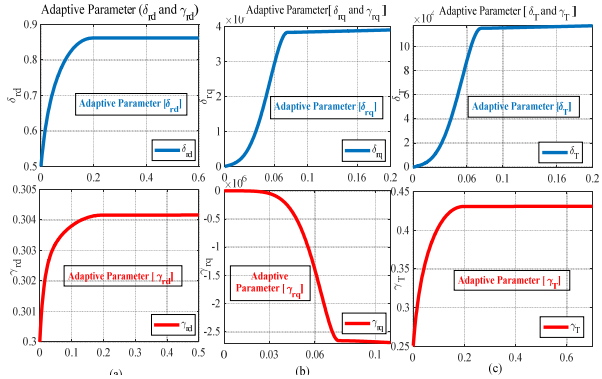

Fig.7. Adaptive parameters, Generator currents (δ_{rd} , γ_{rd})(a), Generator currents (δ_{rq} , γ_{rq}) (b)and (δ_T , γ_T)(c).

In examining the results obtained from the simulation, it can be seen that the FFTASM control approach has a better performance for the turbine rotor speed and the DFIG. Fig.2 to Fig.7 show that the FFTASM controller increases tracking accuracy and performs power adjustment well. In addition, the tracking error is tiny and close to zero.

The simulation results confirm the reliability of the new FFTASM control, as the results show consistency, high tracking accuracy, and power factor proportional to wind speed and specific speed. Active and reactive power tracking errors are very small and increase the system's robustness.

5.1. A Comparison with a related reference

Recently in [45], control of wind power based on adaptive sliding mode control has been proposed. We compared our proposed controller to the designed controller in [45]. The authors in [45] have assumed that the upper bound of the system perturbations is fixed and known, while we considered that the upper bound is not only a nonlinear function but also the coefficients of this function are unknown.

In [45], contrary to equation (39), the reaching law has been defined as $\dot{s} = -\rho s - \hat{\mu} sat(s)$, where the parameter is obtained via an adaptive law $\dot{\hat{\mu}} = n|s|$. The simulation results of applying the adaptive sliding mode controller in [45] into our wind turbine system with same parameters as in Table 1 and external disturbance and model uncertainties like (76) are shown in Fig.8- Fig.10.

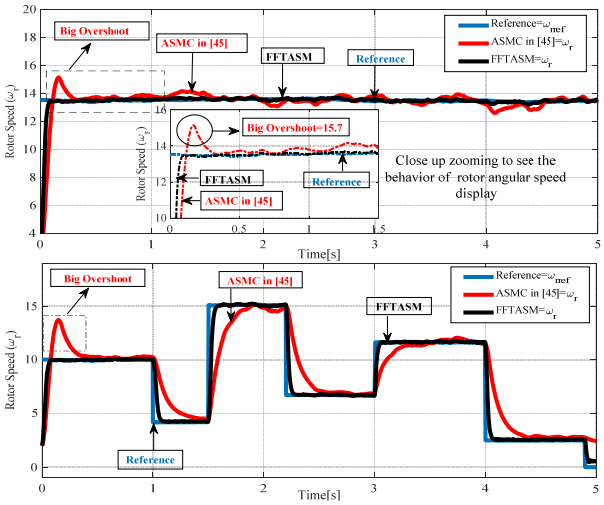

Fig. 8. The behavior of the angular speed of wind turbine rotor based on FFTASM target controller approach compared to ASMC controller based on step dynamic signal profiles(a)and step sequence dynamic signal profile(b)

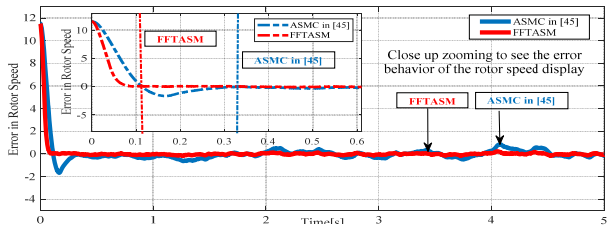

Fig. 9. The error behavior of the speed of wind turbine rotor on FFTASM control approach compared to ASMC controller.

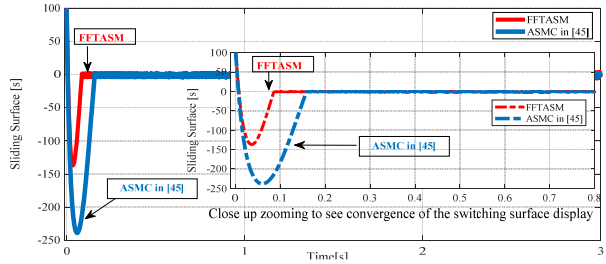

Fig. 10. The behavior of the FFTASM target control approach in the finite

time convergence of the switching surface compared to the ASMC controller in [45].

A comparison of Fig. 8, Fig. 9, and Fig. 10, clearly shows that in the presence of uncertainties and perturbations, the adaptive sliding mode controller designed in [45] does not provide an acceptable convergence in turbine speed. In addition, the error in Fig. 8, has a big overshoot and is slow to converge to zero. Also, the sliding surface in Fig. 10 practically does not converge to origin in addition to the existing chattering. All of this indicates a lack of convergence in a finite time.

According to the results of the comparison, the designed control approach law based on FFTASM has performed much better than the reference controller [45] in the convergence of basic parameters such as turbine rotor speed error and the tracking of the angular rotor speed with respect to different target profiles, as well as achieving fast finite-time convergence in the presence of unknown unlimited perturbations dependent on the dynamical state variables of the model.

The new control approach (FFTASM) presented in Theorems 1 and 2, has been able to lead to an improvement in the tracking performance, reducing the chattering effect, stability and coping with the unlimited changes of modeling uncertainty and external disturbances, and most importantly, leads to the convergence of error components in the system in a limited time.

Table 2 shows a comparison of the statistical indicators of the FFTASM control approach and the ASMC controller such as the values of RMS and NRMS of the rotor angular speed error for the proposed controller are 1.8454 and 0.1528, respectively. The similar results of adaptive controller are 2.1457 and 0.2941. Therefore, the suggested controller results are better than the adaptive controller in [45] also in the sense of RMS and NRMS indicators.

Table 2: FFTASM and ASMC statistical indices

Description	**Parameters**	**FFTASM**	**ASMC In [45]**
Rotor angular Speed RMS	RMS	1.8454	2.1457
Rotor angular Speed NRMS	NRMS	0.1528	0.2941
Rotor angular Speed overshoot	OSH	0.0207	1.6445
Rotor angular Speed rise Time (s)	RT	0.0785	0.1129
Switching Surface Time (s)	SST	0.8s	1.8s
Error Settling Time (s)	EST	0.9s	3s

6. CONCLUSION

A fast and robust-adaptive finite-time sliding mode controller is proposed in this paper to control a perturbed DFIG-based wind turbine, which is exposed to unbounded disturbances and uncertainties. To do this, in Zone II of WECS, a new robust-adaptive fast finite time SMC (FFTASM) is designed for the nonlinear first order model of DFIG system to maximize the produced power in the presence of modeling uncertainties and external disturbances with an unknown functional upper bound. The designed control approach has excellent robustness and stability against parametric uncertainties and unlimited external disturbances. Also, in Zone III of wind turbine, a pitch angle control method is presented using another FFTASM controller in order to tracking the desired speed in finite time in the presence of mentioned perturbations for the nonlinear second order model of pitch angle system. At the same time, in both controllers, unknown coefficients of the functional upper bound of the perturbations are estimated via some stable adaptive laws. A new idea for reducing the effect of chattering is also proposed in this paper. Finally, the results of simulations and statistical indicators are presented to confirm the effectiveness and superiority of the proposed FFTASM approach compared to some recent references.

Data availability statement (DAS)

Data sharing is not applicable to this article as no new data were created or analysed in this study.

Disclosure statement

No potential conflict of interest was reported by the authors.

REFERENCES

[1]H. Fathabadi. Optimal control of a wind energy conversion system and a wind turbine. Optimal *control and Application methods*.2018. 39(4):1354-1370. 10.1002/oca.2415

[2] H. Gouabi, A. Hazzab, M. Habbab, M. Rezkallah and A. Chandra: Experimental implementation of a novel scheduling algorithm for adaptive and modified P&O MPPT controller using fuzzy logic for WECS. *International Journal of Adaptive Control and Signal Processing*. 2021.35(9):1732-1753.doi.org/10.1002/acs.3288

[3] S. M. Mehdizadeh Moghadam, E. Alibeiki1 and A. Khosravi .Modelling and Control of 6MG Siemens Wind Turbine Blades Angle and Rotor Speed. *International Journal on Electrical Engineering and Informatics*.2019.22(2):80-100.10.15676/ijeei.2019.11.1.5

[4] T.Samina, S.Ramalyer, A.B.Beevi . Dynamic behavior

of wind driven doubly fed induction generator with rotor side control for wind power application. In:*2017 International Conference on Energy, Communication, Data Analytics and Soft Computing (ICECDS)*,Chennai, India, 01-02 August 2017 ,pp. 2470-2475.10.1109/ICECDS.2017.8389896.

[5] X. Zhang, H. Liu, Y. Fu and Y. Li. Virtual Shaft Control of DFIG-Based Wind Turbines for Power Oscillation Suppression. *IEEE Transactions on Sustainable Energy*. 2022. 13(4): 2316-2330. 10.1109/TSTE.2022.3194164

[6] El. Mourabit Y, Derouich A, Allouhi A, El Ghzizal A, El Ouanjli N, Zamzoumyes. Sustainable production of wind energy in the main Morocco's sites using permanent magnet synchronous generators. *International Transaction Electrical Energy Systems*.2020.30(6):12390.10.1002/2050-7038.12390

[7] L.Ouada, S.Benaggoune and S.Belkacem. Neuro- Fuzzy sliding mode controller based on brushless doubly fed induction generator , *International Journal of Engineering TRANSACTIONS B: Applications*. 2020.33(2): 248-256. 10.5829/IJE.2020.33.02B.09.

[8] A. D., Bebars, A.A. Eladl, G. M. Abdulsalam . Internal electrical fault detection techniques in DFIG-based wind turbines: a review. *Protection and Control of Modern Power Systems*.2022.7(18):236-251.10.1186/s41601-022-00236-z.

[9] J. Shair, X. Xie, J. Yang, J. Li and H. Li . Adaptive Damping Control of Sub synchronous Oscillation in DFIG-Based Wind Farms Connected to Series-Compensated Network. *IEEE Transactions on Power Delivery* 2022.37(2):1036-1049.10.1109/TPWRD.2021.3076053.

[10] M.J.Morshed.A.Fekin.Design of a chattering-free integral terminal sliding mode approach for DFIG-based wind energy system, *Optimal control and Application methods*.2020.41(5): 1718-1734.10.1002/oca.2635.

[11] LN Huang,B yang,Xs Zhang,Lf Yin,TY u,ZH Fang .Optimal power tracking of doubly fed induction generator-based wind turbine using swarm moth-flame optimizer. *Transactions of the Institute of Measurement and Control*.2017.41(6):1491-1503.10.1177/0142331217712091.

[12] D.Yu,Y.Mao,B.Gu,S.Nojavan,M.Nasseri.A new LQG optimal control strategy applied on a hybrid wind turbine solid oxide fuel cell. In the present of the interval uncertainties. *Sustainable Energy*, Grids and Network.2021. 21(4):100-296.10.1016/j.segan.2019.100296.

[13] P. Li, J. Wang , L. Xiong, M. Ma, M. W Khan, and S. Huang.Robust finite-time controller for damping of subsynchronous resonance in doubly fed induction generator wind farm. *Journal of Vibration and Control*.2020.27(1-2):129-139.10.1177/1077546320924490.

[14] P. P. Pradhan, B. Subudhi and A. Ghosh. A Robust Multiloop Disturbance Rejection Controller for a Doubly Fed Induction Generator-Based Wind Energy Conversion System .*in IEEE Journal of Emerging and Selected Topics in Power Electronics*.2022.10(5):6266-6273. 10.1109/JESTPE.2022.3155561.

[15]S.Hamideh Sedigh,Ziyabari , M. AliyariShoorehdeli,and M. Karimirad.Robust fault estimation of a blade pitch and drivetrain system in wind turbine model. *Journal of Vibration and Control*.2021.27(3-4)277-294.10.1177/1077546320926274.

[16] A.Asgharnia,R.Shahnazi,A. Jamali .Performance and robustness of optimal fractional fuzzy PID controller for pitch controller of a wind turbine using chaotic optimization algorithms , *ISA Transaction* .2018.79(6):27-44.10.1016/j.isatra.2018.04.016.

[17] B. Bossoufi. Rooted Tree Optimization for the Backstepping Power Control of a Doubly Fed Induction Generator Wind Turbine., *in IEEE Access*. 2021.9(2):26512-26522.10.1109/ACCESS.2021.3057123.

[18] Sh. G. Karad and R. Thakur. Enhanced control of doubly fed induction generator based wind turbine system using soft computing assisted fractional order controller. *Renewable Energy Focus*2022.43(2):291-308.10.1016/j.ref.2022.10.006.

[19] Bossanyi E, Fleming P, Wright A.Validation of individual pitch control by field tests on two- and three-bladed wind turbines. *IEEE Transaction Control System Technology*.2014.21(4):1067-78 . 10.1109/TCST.2013.2258345.

[20] J. E. Sierra-García and M. Santos .Improving Wind Turbine Pitch Control by Effective Wind Neuro-Estimators, *IEEE Access*. 2021. 9: 10413-10425 .10.1109/ACCESS.2021.3051063.

[21] R. Prasad and N. P. Padhy.Synergistic Frequency Regulation Control Mechanism for DFIG Wind Turbines with Optimal Pitch Dynamics. *IEEE Transactions on Power Systems*. 2020.35(4): 3181.3191. 10.1109/TPWRS.2020.2967468

[22] H. Chojaa, Derouich, A., Taoussi, M., Zamzoum, O., Yessef, M. Optimization of DFIG wind turbine power quality through adaptive fuzzy control, *Digital Technologies and Applications*.in: ICDTA 2021. In: Lecture Notes in Networks and Systems, 211, Springer. 2021.pp.235-1244.10.1007/978-3-030-73882-2_113.

[23] L. Djilali, A. Badillo-Olvera, Y. Yuliana Rios, H. López-Beltrán and L. Saihi .Neural High Order Sliding Mode Control for Doubly Fed Induction Generator based Wind Turbines. *IEEE Latin America Transactions*. 2022.20(2): 223-232.10.1109/TLA.2022.9661461.

[24] S. M. Mehdizadeh Moghadam, A. R. Khosravi and S. M. Rakhtala Rostami. Design of a Robust Sliding Mode Controller based on Nonlinear Modeling of Variable Speed

Wind Turbine. *Majlesi Journal of Electrical Engineering*. 2017.11(4): 1-9.10.30486/mjee.2024.2000004.1301.

[25] Ali Karami-Mollaee,Ali Asgghar shojaei,Oscar Baram bones,Mohd Fauziothman .Dynamic sliding mode control of pitch blade wind turbine using sliding mode observer ,*Transactions of the Institute of Measurement and Control.* 2022. 44(10): 1491-1503. 10.1177/01423312221099304.

[26] K. Tahir, T. Allaoui, M. Denai, et al .Second-order sliding mode control of wind turbines to enhance the fault-ride through capability under unbalanced grid faults, *International Journal of Adaptive Control and Signal Processing*.2021.49(7): 1959-1986.10.1002/cta.3023.

[27] Aghiles Ardjal ,Rachid Mansouri,Maamar Bettayeb . Fractional sliding mod control of wind turbine for maximum power point tracking , *Transactions of the Institute of Measurement and Control*.2019.41(2):447-457.10.1177/01423312187645.

[28] L. Xiong, Wang, J., Mi, X., Khan, M.W . Fractional order sliding mode based direct power control of grid-connected DFIG. *IEEE Transaction Power System*. 2018.33 (3): 3087-3096.10.1109/TPWRS.2017.2761815.

[29] H. Zhang and T. Wang. Finite-Time Sliding Mode Control for Uncertain Neutral Systems With Time Delays, *IEEE Access*. 2021.9: 140446-140455. 10.1109/ACCESS.2021.3119628.

[30] Z.Yan,S.Zhong,S.He. Finite-time H2/Hinf control for linear Ito stochastic Markovian jumper systems with Brownian motion and Poisson jumper, *System and Control Letters*.2022.165(4):105285.10.1016/j.sysconle.2022.105285.

[31] Patnaik, R.K., Dash, P.K. & Mishra, S.P. Adaptive third order terminal sliding mode power control of DFIG based wind farm for power system stabilization, *International Journal of Dynamics and Control*.2020. 8(4):629–643.10.1007/s40435-019-00567-0.

[32] M. J. Morshed and A. Fekih . Second order integral terminal sliding mode control for voltage sag mitigation in DFIG-based wind turbines. In: *IEEE Conference on Control Technology and Applications (CCTA),*Maui,USA,2017. 27-30 August,pp.1724-1736.10.1109/CCTA.2017.8062530.

[35]S.E. Chehaidia, H. Kherfane , H. Cherif , B. Boukhezzar, L. Kadi,H.Chojaa , A.Abderrezak .Robust Nonlinear Terminal Integral Sliding Mode Torque Control for Wind Turbines Considering Uncertainties. *IFAC-PapersOnLine*. 2022.55(12):228-233.10.1016/j.ifacol.2022.07.316.

[34] M. Ali, S. M. Amrr and M. Khalid. Speed control of a wind turbine–driven doubly fed induction generator using sliding mode technique with practical finite□time stability, *Frontiers in Energy Research*.2022. 10(2): 970755 .10.3389/fenrg.2022.970755.

[35] L. Haitao and T. Zhang .Adaptive Neural Network Finite-Time Control for Uncertain Robotic Manipulators, *Journal of Intelligent & Robotic Systems*. 2014.75(4): 363-377.10.1007/s10846-013-9888-5.

[36] Y. Wang, L. Gu, Y. Xu and X. Cao. Practical Tracking Control of Robot Manipulators with Continuous Fractional-Order Nonsingular Terminal Sliding Mode , *IEEE Transactions on industrial electronics*, 20156.63(10): 6194-6204.10.1109/TIE.2016.2569454.

[37] Hong,Y., Huang, J., & Xu,Y. On an output finite-time stabilization problem, *IEEE Transactions on Automatic Control*, 2001.46(2):305-309.10.1109/9.905699.

[38]S. Labdai, N. Bounar , A. Boulkroune , B. Hemici , L. Nezli.Artificial neural network-based adaptive control for a DFIG-based WECS.*ISA Transactions*.2022. 128(b):171-180.10.1016/j.isatra.2021.11.045.

[39] M. Karim, M. Taoussi, H. Aroussi, M. Bouderbala, S. Motahhir, M. Baïlo Camara.DSPACE-based implementation for observer backstepping power control of DFIG wind turbine. IET *Electric Power Application*.2020.14(12):2395-2403.10.1049/iet-epa.2020.0364.

[40] J. Ma,Z. Song, Y. Zhang, Yu.Zhao, J S. Thorp.Robust Stochastic Stability Analysis Method of DFIG Integration on Power System Considering Virtual Inertia Control. *IEEE Transactions on Power Systems*.2017.32(5):4069-4079.10.1109/TPWRS.2017.2657650.

[41] Y. Yuan, Xu. Chen, J. Tang.Multivariable robust blade pitch control design to reject periodic loads on wind turbines .*Renewable Energy*.2020.146(2):329-341.10.1016/j.renene.2019.06.136.

[42] O. Zamzoum, El Mourabit, Y. Errouha, M. Derouich, A. El Ghzizal, .A power control of variable speed wind turbine based on doubly fed induction generator using indirect field-oriented control with fuzzy logic controllers for performance optimization. *Energy Science Engineering* .2018.6 (5): 408-423.10.1002/ese3.215.

[43] M. N. Soorki and M. S. Tavazoei. Adaptive robust control of fractional-order swarm systems in the presence of model uncertainties and external disturbances, *IET Control Theory & Applications*.2018.12(7):961-969.10.1049/iet-cta.2017.0035.

[44] Si-Ammour, A, Denounce, S., Bettayeb, M. A sliding mode control for linear fractional systems with input and state delays, *Communications in Nonlinear Science and Numerical Simulation* .2018.14(5):2310–2318.10.1016/j.cnsns.2008.05.011.

[45] Y. Mi, Y. Song, Y. Fu, X. Su, C. Wang and J. Wang. Frequency and Voltage Coordinated Control for Isolated Wind–Diesel Power System Based on Adaptive Sliding Mode and Disturbance Observer, in *IEEE Transactions on Sustainable Energy*. 2019.10(4):2075-2083.10.1109/TSTE.2018.2878470.